# REACTION SINTERING OF METAL-CERAMIC AlSi-$Al_2O_3$ COMPOSITES MANUFACTURED BY BINDER JETTING ADDITIVE MANUFACTURING PROCESS

Vadim SUFIIAROV, Artem KANTYUKOV, Igor POLOZOV

*Peter the Great St. Petersburg Polytechnic University, St. Petersburg, Russia, vadim.spbstu@yandex.ru*

https://doi.org/10.37904/metal.2020.3618

**Abstract**

Metal-ceramic composites are attractive materials for various applications due to their high specific strength, wear resistance, thermal stability, and good high-temperature mechanical properties. Binder jetting additive manufacturing is a promising way of manufacturing metal-ceramic composite parts with complex geometry. In this work, $Al_2O_3$ - Si powder blend was used to produce metal-ceramic green-parts by binder jetting process. The green-parts were then subjected to reaction sintering and subsequent liquid metal infiltration with aluminum alloy at 1200 ºC. The microstructure and phase composition of the obtained samples were studied using scanning electron microscopy and X-Ray diffraction analysis. Mechanical properties were evaluated using microhardness measurements and compressive tests.

**Keywords:** Additive manufacturing, metal-ceramic composites, binder jetting, liquid metal infiltration

## 1. INTRODUCTION

Metal-ceramic composites with a ceramic material as a matrix are of great interest for various applications. These systems are valued for their low weight, thermal and mechanical properties at high temperatures. These composites are used in the manufacture of cutting tools, dies, gas turbine parts, high-pressure heat exchangers and ballistic armor, and much more [1-3]. Composites are usually reinforced with other ceramics, where, for example, $SiO_2$ is added to the matrix of $Al_2O_3$, in these cases, the presence of the reinforcement phase deflects cracks during their formation, allowing the material to demonstrate excellent mechanical properties. Also, they usually have at least one penetrating material, which is the metal phase, due to the ability of the molten metal to infiltrate the porous structure.

One of the most common systems is the $Al_2O_3$ - Al system due to its lightweight and high strength properties. These composites can be manufactured using a large number of technologies, which include: a directed metal oxidation process (DIMOX) [4] using the Lanoxide method using an oxide displacement reaction, also known as a reactive metal penetration process (RMP) [5], injection molding [6], gas pressure infiltration [7], and self-propagating high-temperature synthesis [8]. Based on these methods, the RMP process is widely used because it uses a natural reduction reaction between molten metal (Al) and a ceramic material ($SiO_2$).

The greatest difficulty in the production of cermet by traditional methods is the manufacture of products of complex shape, such parts are usually made by hand, which leads to low repeatability, high cost and production time.

Additive Manufacturing (AM) can be used to fabricate complex-shaped parts from various materials [9,10]. AM are a group of technologies involving the manufacturing of a product according to a digital model by the method of layer-by-layer addition of material. Due to the fact that the manufacturing of the product takes place in layers, it is possible to produce parts with complex geometry with virtually no shape limitation in less time. Among AM methods, Binder Jetting process (BJ) is suitable for fabrication of parts using metal alloys, ceramic and intermetallic materials [11-13]. In this method, a liquid binder material is applied to the powder layer in places

corresponding to the section of the part followed by curing the binder. Then, the green part can be either sintered or infiltrated with another material to achieve a dense structure [14].

This paper is devoted to the study of the manufacturing of ceramic-metal composites using Binder Jetting method from a 60$Al_2O_3$-40Si (wt%) powder blend. Two post-processing techniques were evaluated for the fabricated green-parts: sintering and liquid metal infiltration. Microstructure, chemical homogeneity, and microhardness of the samples were evaluated.

## 2. MATERIALS AND METHODS

Spherical powder of $Al_2O_3$ (corundum, purity 99,9%) and irregular powder of Si (99%) were used as starting powders for the preparation of powder blends of 60 $Al_2O_3$-40Si (wt%). In a gravity mixer, 60 % of the original corundum powder was mixed by weight with 40% of silicon for 24 hours to obtain a uniform mixture. Particle size distribution of the corundum powder is characterized by the following values of the parameters $d_{10}$ = 28.3 μm, $d_{50}$ = 59.2 μm and $d_{90}$ = 109.8 μm and SEM-images are shown in the **Figure 1 a**. Particle size distribution of silicon: $d_{10}$ = 4.9 μm, $d_{50}$ = 52.3 μm and $d_{90}$ = 127.7 μm and SEM-images are shown in the **Figure 1 b**. Particle size distribution of the powder was measured by laser diffraction technique with Analysette 22 NanoTec.

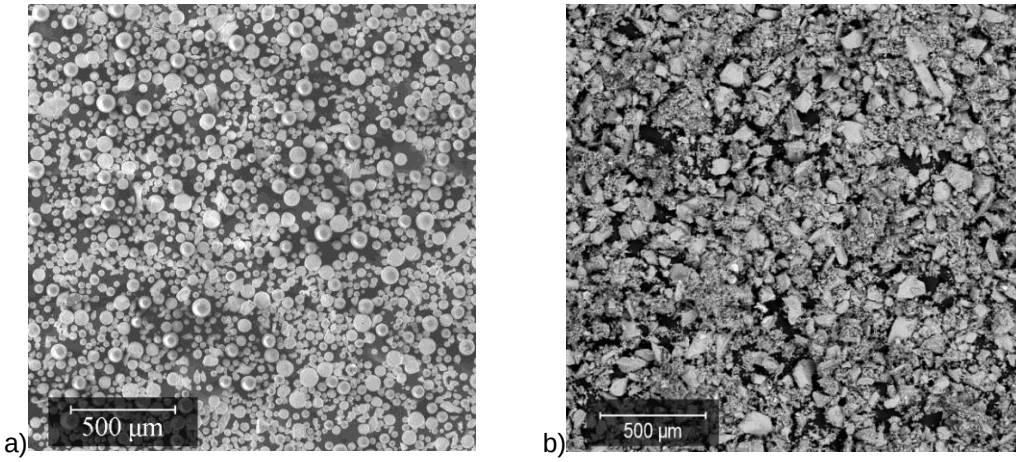


**Figure 1** SEM-images of initial powders: $Al_2O_3$ (a), Si (b)

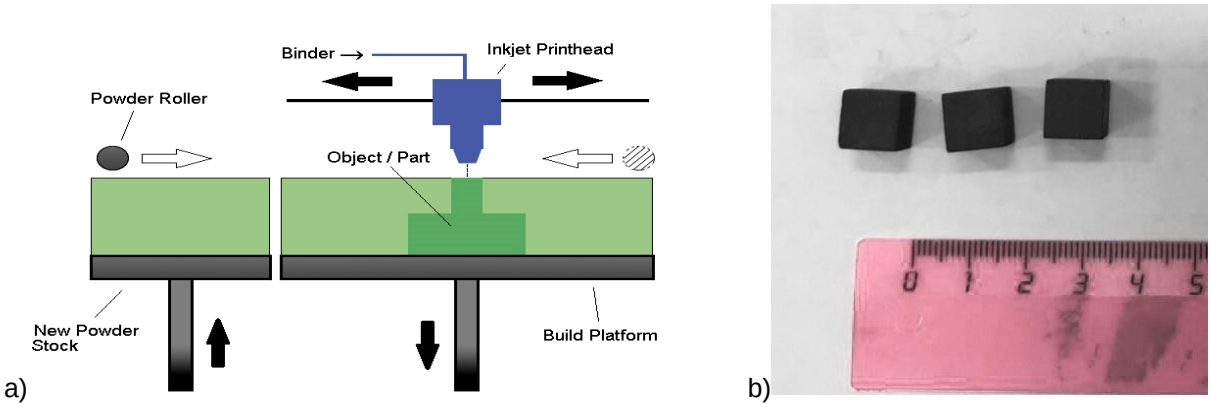


**Figure 2** The scheme of a binder jetting process (a), the as-printed sample from mixtures of 60$Al_2O_3$-40Si (b)

The ExOne Innovent BJ 3D-printer and aqueous binder (ExOne) were used to build samples of 10 mm x 10 mm x 10 mm in size with the following printing parameters: 40% binder saturation, 40 s dry time, 5 mm/s recoat speed, 100 μm layer thickness. The scheme of a binder jetting process is shown at **Figure 2 a**. After completion

of the layer-by-layer synthesis, the working bath together with the samples was placed in a Yamato DX412C thermal furnace, where it was kept at a temperature of 180–190 °C for 3-5 hours to cure the binder material. **Figure 2 b** shows the image of as-printed samples from mixtures of 60 $Al_2O_3$-40 Si after curing the binder.

Then the parts were removed from the furnace, and the excess powder was brushed off to remove the cured part. At this point, the particles were bonded to each other by a cured binder. To obtain a dense part, the samples were subjected to a subsequent sintering cycle. Sintering was carried out stepwise, at first the samples were heated at a speed of 5 °C/min to 600 °C to remove the binder material, then at a speed of 10 °C/min they were heated to 1500-1600 °C and held for 1-4 hours. The sintering process was carried out in air to oxidize silicon in a high-temperature KJ-1700X furnace.

Then the sintered blanks were infiltrated by the method of penetration of a reactive metal. Samples were immersed in excess molten aluminum and held for approximately 16 hours at 1200 °C.

The microstructure of the samples was studied using TESCAN Mira 3 LMU scanning electron microscope (SEM)

The phase composition was analyzed with a Bruker D8 Advance X-ray diffraction (XRD) meter using CuKα irradiation. The microhardness of the samples was measured using Buehler VH1150 tester with 1 kg loading and 10 s dwelling time. Thermogravimetric analysis (TGA) was carried out with TA Instruments TGA Q5000.

## 3. RESULTS AND DISCUSSION

To evaluate the curing characteristics of the binder, TGA analysis was performed by heating the binder sample to 600 °C with a heating rate of 1 °C/min. The aqueous binder consists of a mixture: demineralized water 70%, ethanediol 5-10%, 2-butoxyethanol 15-20%. **Figure 3** shows the change in binder mass as a function of temperature. After heating above 100 °C, the mass decreases sharply and levels off at a temperature of about 175-180 °C, which is associated with the evaporation of the aqueous component. When the binder was heated to 180 °C, the mass of the sample decreased by 85%. In the temperature range 180–400 °C, the mass practically did not change. Above 400 °C, the mass decreased even more, and at 400 °C it was 10% of the initial mass and 0.1% at 450 °C.

In the sintering step, the binder was burned to leave a consolidated sample. Above 600 °C, the aqua-based binder was completely removed with a minimum of carbon content.

After curing, the green samples were sintered at 1600 °C for 4 hours. Preliminary experiments showed that lower sintering temperatures and shorter holding times did not provide sufficient strength of the samples.

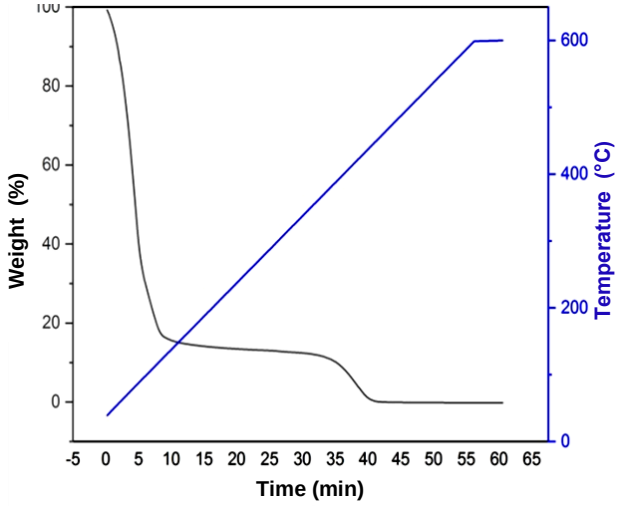


**Figure 3** Mass change of the aqua binder depending on temperature

At a sintering temperature of 1500 °C and a holding time of 2 hours, only the initial stages of liquid phase sintering are observed (**Figure 4**). Silicon began to melt and wet the alumina particles, however, the process of consolidation of individual powder particles into a dense structure did not occur.

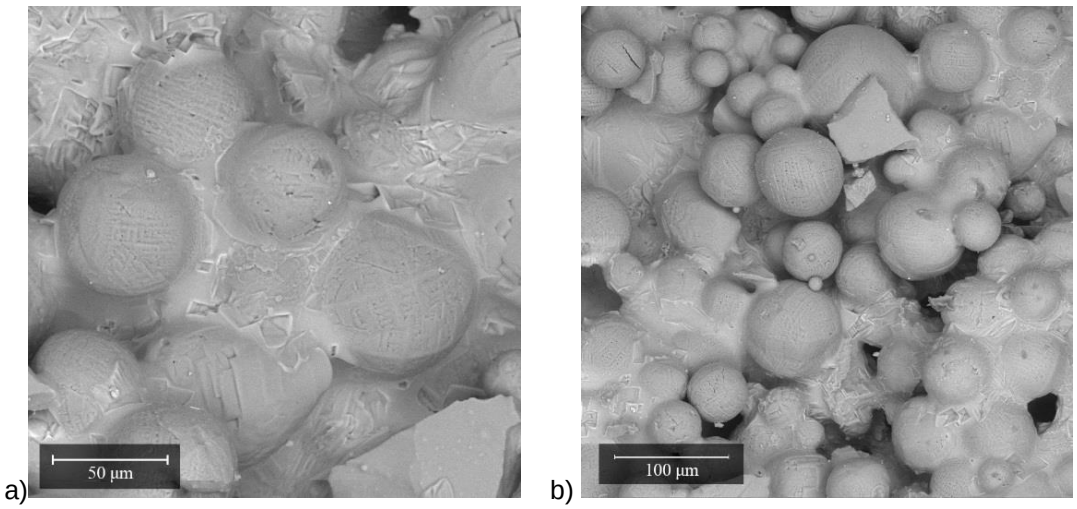


**Figure 4** SEM-images of $60Al_2O_3$-40Si samples after sintering at 1500 °C for 2h

Cubic samples were used to measure shrinkage: volumetric shrinkage was 10% when sintering at 1600 °C for 4 hours, and at temperatures below 1600 °C, no shrinkage of the samples was observed. The density of the samples after sintering at 1600 ºC for 4h was 2.04 g/cm$^3$, which corresponds to 61.9% of the theoretical density of the composite material.

The image of the sample structure after sintering at 1600 °C for 4 hours is shown in **Figure 5**. The initial powder form of the particles was not left, the pores have a chaotic distribution, ordering in their shape and location is not observed. In this case, X-ray phase analysis (**Figure 6**) showed that sintering produces mullite, which demonstrates the interaction of oxygen with silicon and alumina.

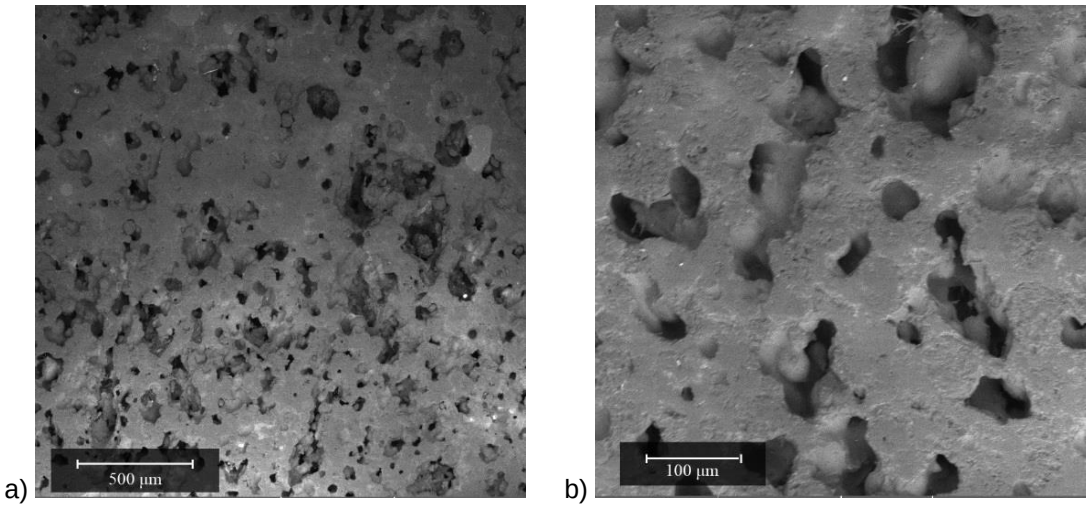


**Figure 5** SEM-images of $60Al_2O_3$-40Si sample after sintering at 1600 °C for 4h

Studies of compressive strength showed that the maximum strength value was 31 MPa. Such a low value is caused by the high porosity of the samples. Microhardness could not be measured due to the large number of pores, the sample crumbled upon exposure to a core of 1 kg and no indent was visible.

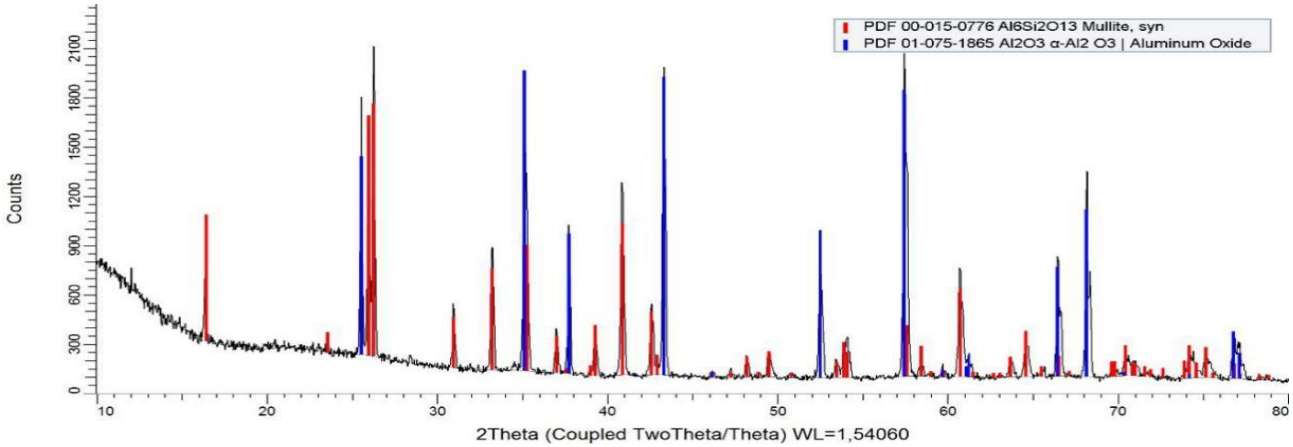


**Figure 6** The XRD pattern of $60Al_2O_3$-40Si sample during sintering at 1600 °C for 4h

For the infiltration process, samples of 60%$Al_2O_3$-40%Si, previously sintered at a temperature of 1600 °C for 4 hours, were immersed in molten aluminum. The experiment was carried out at 1200 °C for 16 hours. The interaction between mullite and aluminum melt proceeds according to the following reaction (1) [15]:

$$3\ Al_6Si_2O_{13} + (8+x)\ Al \rightarrow 13\ Al_2O_3 + (x)\ Al + 6\ Si \quad (1)$$

In **Figure 7**, taken by SEM it can be seen that the inner surface has a dense structure, but there are a small number of randomly distributed pores. Some defects were caused by grinding and polishing. When one material is harder (ceramic) acts on a more plastic (aluminum alloy)

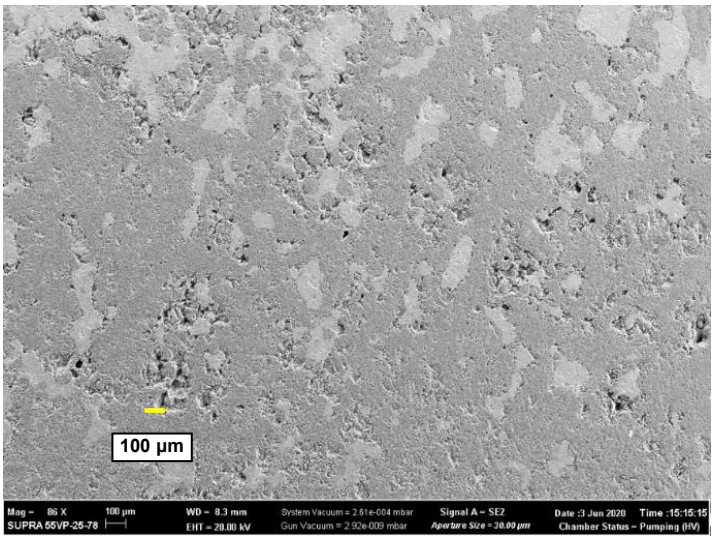


**Figure 7** SEM-image of cross section $60Al_2O_3$-40Si sample after aluminum infiltration

The density of the samples after infiltration with aluminum was 97% of the theoretical density of the composite material.

Chemical mapping was made (**Figure 8**), it shows that samples have a chemical heterogeneity. As can be seen in **Figure 8**, there are three phases - silicon, aluminum oxide and aluminum, which is confirmed by X-ray diffraction patterns (**Figure 9**).

Also, this inhomogeneity determined in the measurement of microhardness, where zones of aluminum oxide have values 800 - 1200 HV, and zones of aluminum alloy are in the range of 300 – 400 HV.

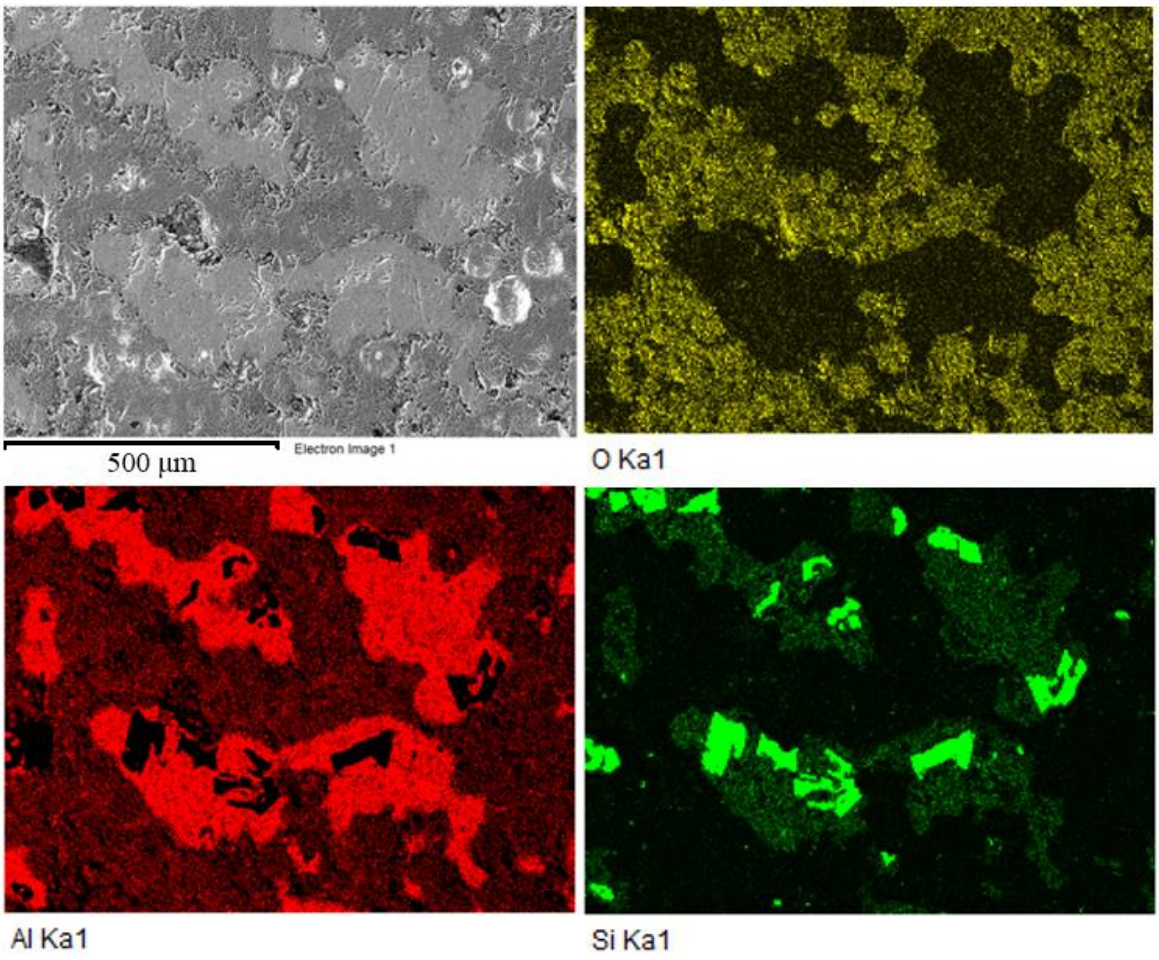


**Figure 8** Chemical maps of the $60Al_2O_3$-40Si sample after metal infiltration with the local chemical composition (gray) and element distribution for O (yellow), Si (green) and Al (red)

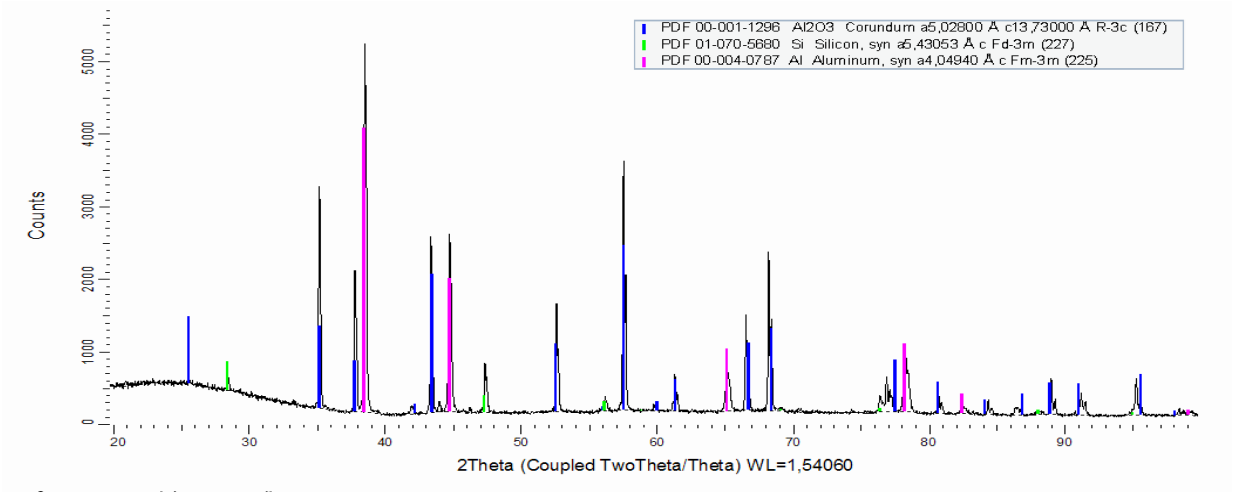


**Figure 9** The XRD pattern of $60Al_2O_3$-40Si sample after metal infiltration

Combining chemical maps of aluminum, silicon and oxygen to one image (**Figure 10**), it can be found that silicon is surrounded by aluminum. This is due to the fact that in hypereutectic Al-Si alloy, silicon have form of polyhedral crystals.

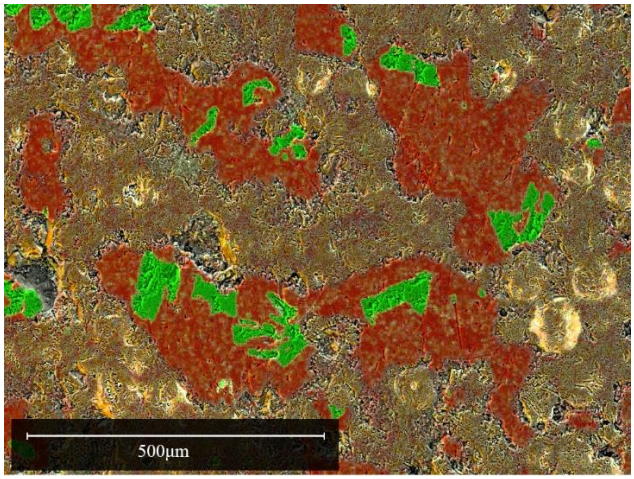


**Figure 10** Chemical map of elements distribution for O (yellow), Si (green) and Al (red) in 60$Al_2O_3$-40Si sample after metal infiltration

## 4. CONCLUSIONS

In this paper, Binder Jetting AM process, reaction sintering and reaction melt infiltration were used to fabricate metal-ceramic composite consisting of $Al_2O_3$ ceramic and Al alloy. Liquid metal infiltration was successfully applied to $Al_2O_3$-Si green parts to obtain dense samples. As the result of reactive infiltration, reactions occurred with the formation of alumina and aluminum alloy. Due to the heterogeneity of the chemical composition, the microhardness varied in the range of 800–1200 HV and 300–400 HV, respectively.

## ACKNOWLEDGEMENTS

***This research was supported by Russian Science Foundation grant (project No 18-79-00207).***

## REFERENCES

[1] CLAUSSEN, N., WU, S., HOLZ, D. Reaction bonding of aluminum oxide (RBAO) composites: Processing, reaction mechanisms and properties. *Journal of the European Ceramic Society.* 1994, vol. 14, pp. 97-109.

[2] SHAUN, P.G., SHEEDY, P.M., HUGO, C., CHAN, H.M. Controlled firing of reaction-bonded aluminum oxide (RBAO) ceramics: Part II, Experimental results. *J. Am. Ceram. Soc.* 1999, vol. 82, pp. 909–1015

[3] CLAUSSEN, N., WU, S., HOLZ, D., SCHEPPOKAT, S. Effect of processing parameters on phase and microstructure evolution in RBAO. *Ceramics Am Cerunr. Jot*. 1994, vol. 71, pp. 2509-2517

[4] KUMAR**,** S.S., DEVAIAH, M. M., BAI, V.S., RAJASEKHARAN, T. Mechanical properties of $SiC_p/Al_2O_3$ ceramic matrix composites prepared by directed oxidation of an aluminum alloy. *Ceramics International*. 2012, vol. 38, pp. 1139-1147.

[5] MANFREDI**,** D., PAVESE, M., BIAMINO, S., FINO, P., C BADINI, C. NiAl(Si)/$Al_2O_3$ co-continuous composites by double reactive metal penetration into silica preforms. *Intermetallics*. 2008, vol. 16, pp. 580-583.

[6] EGÉSZ, Á., GÖMZE, L.A., Qualification methods of $Al_2O_3$ injection molding raw materials. *Journal of Physics: Conference Series.* 2013, vol. 602, pp. 7 – 11

[7] DEMIR, A., ALTINKOK, N., Effect of gas pressure infiltration on microstructure and bending strength of porous $Al_2O_3$/SiC-reinforced aluminum matrix composites. *Composites Science and Technology*. 2004, vol. 16, pp. 2067-2074

[8] PATHAK, L.C., BANDYOPADHYAY, D., SRIKANTH, S., DAS, S.K., RAMACHANDRARAO, P. Effect of heating rates on the synthesis of $Al_2O_3$–SiC composites by the self-propagating high-temperature synthesis (SHS) technique . *Journal of the American Ceramic Society.* 2001, vol. 84, pp. 915-920

[9] AGAPOVICHEV, A.V., KOKAREVA, V.V., SMELOV, V.G, SOTOV, A.V. Selective laser melting of titanium alloy: investigation of mechanical properties and microstructure. *IOP Conf. Series: Materials Science and Engineering* 2016, vol. 105, p. 012031

[10] SOTOV, A.V., AGAPOVICHEV, A.V., SMELOV, V.G., KOKAREVA, V.V., ZENINA, M.V. Investigation of the Ni-Co-Cr alloy microstructure for the manufacturing of combustion chamber GTE by selective laser melting. *International Journal of Advanced Manufacturing Technology.* 2019, vol. 101, pp. 9-12.

[11] SUFIIAROV, V., POLOZOV, I., KANTYKOV, A., KHAIDOROV, A. Binder jetting additive manufacturing of 420 stainless steel: Densification during sintering and effect of heat treatment on microstructure and hardness *Materials Today: Proceedings,* 2020.

[12] POLOZOV, I., SUFIIAROV, V., SHAMSHURIN, A. Synthesis of titanium orthorhombic alloy using binder jetting additive manufacturing. *Materials Letters.* 2019, vol. 243, pp. 88-91.

[13] MOSTAFAEI, A. ELLIOTT, A.M., BARNES J.E.,CRAMER, C.L. Binder jet 3D printing–process parameters, materials, properties, and challenges. *Progress in Materials Science.* 2020.

[14] TOFAIL, A.M., ELIAS, P., BANDYOPADHYAY, K.A. Additive manufacturing: scientific and technological challenges, market uptake and opportunities. *Materials Today.* 2018, vol. 21 pp. 22-37.

[15] NAGA, S.M., EL-MAGHRABY, A.A., EL-RAFEI, A.M., WINDSHEIMER, H., GREIL, P. Reactive infiltration of porous mullite bodies by molten aluminum alloy. In *Proc. 10th ECerS Conf.,* 2007 pp. 1121-1125.